Development of a mathematical model describing hydrolysis and co-fermentation of C6 and C5 sugars

Morales Rodriguez, Ricardo; Gernaey, Krist; Meyer, Anne S.; Sin, Gürkan

Published in:
2. International Symposium on Sustainable Chemical Product and Process Engineering

Publication date:
2010

Development of a mathematical model describing hydrolysis and co-fermentation of C6 and C5 sugars

MORALES-RODRIGUEZ Ricardo[a], GERNAEY Krist V.[b], MEYER Anne S.[c] and SIN Gürkan[a]*

[a] CAPEC, [b] PROCESS & [c] BIOENG, Department of Chemical and Biochemical Engineering, Technical University of Denmark, DK-2800 Lyngby, Denmark

Abstract Reliable production of biofuels and specifically bioethanol has attracted a significant amount of research recently. Within this context, this study deals with dynamic simulation of bioethanol production processes and in particular aims at developing a mathematical model for describing simultaneous saccharification and co-fermentation (SSCF) of C6 and C5 sugars. Model construction has been carried out by combining existing mathematical models for enzymatic hydrolysis on the one hand and co-fermentation on the other hand. An inhibition of ethanol on cellulose conversion was introduced in order to increase the degree of reliability. The mathematical model for the SSCF has been tested for a modified version of the process flowsheet proposed by the National Renewable Energy Laboratory (NREL). The model can now be used to evaluate different process configurations for 2G bioethanol production using corn stover as a feedstock.

Keywords bioethanol, second generation, dynamic modeling, plant-wide, SSCF, corn stover.

1 INTRODUCTION

One of the major areas of research is the development of sustainable products-processes particularly aiming at zero emission and reduction of the impact on global warming. Achieving these targets requires increasingly efficient energy production and expanded development of alternative sources of energy supplies that have low greenhouse-gas emissions [1]. Biofuels production from lignocellulosic biomass is one of the alternative technologies that is often studied, and has different process routes such as biochemical versus physical/chemical conversion [2]. The conventional process flowsheet for bioethanol production involves different unit operations such as, physical/chemical pretreatment, enzymatic hydrolysis, fermentation (or simultaneous saccharification and fermentation), and

* Corresponding author. Gürkan Sin, gsi@kt.dtu.dk. Tel.: +45 4525 2806, fax: +45 4593 2906

several downstream processes. One of the main problems is that the transfer of these processes from proof-of-concept to industrial scale is still mainly done on an empirical basis (e.g. experimentally-based) that is typically inefficient and costly in terms of time and resources.

This study aims at the development of a mathematical model for simultaneous saccharification and fermentation (SSCF) of pentose and hexose sugars from a lignocellulosic feedstock. The main challenge was to combine mathematical models describing the involved steps separately, i.e. enzymatic hydrolysis for saccharification on the one hand, and co-fermentation on the other hand. The proposed mathematical model for the SSCF unit has been tested by performing a dynamic simulation of the process configuration for the 2nd generation (2G) bioethanol production process presented in an NREL report [3], where key unit operations include diluted acid pretreatment, on-site cellulase production, simultaneous saccharification and fermentation (hexoses), separate fermentation of pentose sugars, and downstream processes. Matlab/Simulink was used as the model development and simulation platform. The SSCF model was then evaluated within a modified NREL process configuration involving a combination of pretreatment and SSCF units using corn stover as a feedstock. It is important to highlight that other woody or fibrous feedstock (such as, switchgrass, wheat straw, woodchips) can be used employing the corresponding biomass composition.

2 MATHEMATICAL MODELS FOR SSCF UNIT OPERATION

The SSCF mathematical model was built as a combination of the mathematical models to describe the enzymatic hydrolysis [4] on the one hand and co-fermentation [8] on the other hand. In this section, the SSCF model is presented, with special emphasis on the coupling of the individual models via suitable inhibition functions.

2.1. Enzymatic hydrolysis

Among many competing models, the mathematical model developed by Kadam et al. [4] is chosen to describe the enzymatic hydrolysis of lignocellulose. This model has previously been verified and analyzed [5,6,7]. The model to describe the enzymatic hydrolysis of lignocellulosic biomass quantifies the decomposition of the cellulose content in the lignocellulose biomass. This model involves the reaction rates for: (1) the decomposition of cellulose to cellobiose (eq. 1) and glucose (eq. 2) by the action of the enzymes endo-β-1,4-glucanases + exoglucanases; (2) cellobiose hydrolysis into glucose by β-glucosidase enzyme activity (eq. 3). The model furthermore describes enzyme adsorption (eq. 4), the concentrations of free and bound enzyme (eq. 5), the substrate reactivity (eq. 6) and the effect of the temperature on the saccharification by means of the Arrhenius equation (eq. 7). The mathematical model includes the relevant product inhibition phenomena that take place for the enzymatic hydrolysis [4].

Table 1 Mathematical model for the enzymatic hydrolysis [4].

Cellulose to cellobiose, $g/kg \cdot h$	$r_1 = \frac{k_{1r} C_{E_{1B}} R_S C_S}{1 + \frac{C_{G_2}}{K_{1IG2}} + \frac{C_G}{K_{1IG}} + \frac{C_{Xy}}{K_{1IXy}}}$	(1)
Cellulose to glucose , $g/kg \cdot h$	$r_2 = \frac{k_{2r} \left(C_{E_{1B}} + C_{E_{2B}} \right) R_S C_S}{1 + \frac{C_{G_2}}{K_{2IG2}} + \frac{C_G}{K_{2IG}} + \frac{C_{Xy}}{K_{2IXy}}}$	(2)
Cellobiose to glucose, $g/kg \cdot h$	$r_3 = \frac{k_{3r} C_{E_{2F}} C_S}{K_{3M} \left(1 + \frac{C_G}{K_{3IG}} + \frac{C_{Xy}}{K_{3IXy}} \right) + C_{G_2}}$	(3)
Enzyme Adsorption, $g/kg \cdot h$	$C_{E_{iB}} = \frac{E_{i\max} K_{iad} C_{E_{iF}} C_S}{1 + K_{iad} C_{E_{iF}}}$	(4)
Enzyme, g/kg	$C_{E_{Ti}} = C_{E_{Fi}} + C_{E_{Bi}}$	(5)
Substrate reactivity	$R_S = \alpha C_S / S_0$	(6)
Temp. dependence	$k_{ir(T2)} = k_{ir(T1)} e^{-E_{ai}/R \left(1/T1 - 1/T2 \right)}$, $30°C \le T \le 55°C$	(7)

2.2. Co-fermentation

The mathematical model employed in this work for the co-fermentation part in the SSCF model has been adapted from Krishnan et al. [8], and considers

the simultaneous conversion of xylose and glucose to ethanol, also known as a co-fermentation. The co-fermentation model is based on the recombinant *Saccharomyces cerevisiae* strain 1400 (pLNH33).

The mathematical model for co-fermentation involves the reaction rates for: (1) cell growth on glucose (eq. 8) and xylose (eq. 9); (2) the total yeast cell mass production as the average product of the cell growth on glucose and xylose using the mass fraction of these compounds present in the mixture (eq. 10); (3) consumption of glucose (eq. 11) and xylose (eq. 12); (4) formation of ethanol from glucose (eq. 13) and xylose (eq. 14); (5) overall formation of ethanol (eq. 15). The model accounts for both substrate and product inhibition as well as the effect of the inoculum size that is employed for the cultivation.

Table 2 Mathematical model for the co-fermentation [8].

Biomass $_{\text{Glucose}}$, $g/L\cdot h$	$r_4 = \frac{dC_{X_G}}{dt} = \frac{\mu_{\max,G} C_G}{K_{4G} + C_G + \frac{C_G^{\,2}}{K_{4IG}}} \left(1 - \left(\frac{C_{Et_G}}{Et_{\max,G}}\right)^{\beta_G}\right)$	(8)
Biomass $_{\text{Xylose}}$, $g/L\cdot h$	$r_5 = \frac{dC_{X_{Xy}}}{dt} = \frac{\mu_{\max,Xy} C_{Xy}}{K_{5Xy} + C_{Xy} + \frac{C_{Xy}^{\,2}}{K_{5IXy}}} \left(1 - \left(\frac{C_{Et_{Xy}}}{Et_{\max,Xy}}\right)^{\beta_{Xy}}\right)$	(9)
Total biomass, $g/L\cdot h$	$r_{X,TOT} = x_G r_4 + x_{Xy} r_5$	(10)
Glucose, $g/L\cdot h$	$-r_6 = \frac{1}{Y_{Et_G/G}} \frac{dC_{Et_G}}{dt} = \frac{1}{Y_{X_G/G}} \frac{dC_{X_G}}{dt} + m_G C_{X_G}$	(11)
Xylose, $g/L\cdot h$	$-r_7 = \frac{1}{Y_{Et_{Xy}/Xy}} \frac{dC_{Et_{Xy}}}{dt} = \frac{1}{Y_{X_{Xy}/Xy}} \frac{dC_{X_{Xy}}}{dt} + m_{Xy} C_{X_{Xy}}$	(12)
Ethanol $_{\text{Glucose}}$, $g/L\cdot h$	$r_8 = \frac{1}{X_G} \frac{dC_{Et_G}}{dt} = \frac{\nu_{\max,G} C_G}{K'_{8G} + C_G + \frac{C_G^{\,2}}{K'_{8IG}}} \left(1 - \left(\frac{C_{Et_G}}{Et'_{\max,G}}\right)^{\gamma_G}\right)$	(13)
Ethanol $_{\text{Xylose}}$, $g/L\cdot h$	$r_9 = \frac{1}{X_{Xy}} \frac{dC_{Et_{Xy}}}{dt} = \frac{\nu_{\max,Xy} C_{Xy}}{K'_{9Xy} + C_{Xy} + \frac{C_{Xy}^{\,2}}{K'_{9IXy}}} \left(1 - \left(\frac{C_{Et_{Xy}}}{Et'_{\max,Xy}}\right)^{\gamma_{Xy}}\right)$	(14)
Ethanol production, g/L	$r_{Et,TOT} = r_8 + r_9$	(15)

$1 g/kg = 1 g/L$; $\rho_{mixture} = 1\ kg/L$

2.3. Development of the SSCF model

The development of the reaction kinetics for the simultaneous saccharification and co-fermentation (SSCF) model is carried out by combining the models for enzymatic hydrolysis and fermentation described above. One of the main challenges to resolve is the inhibition of the enzymatic hydrolysis step by ethanol. It is known that the presence of ethanol during enzymatic hydrolysis can induce a certain level of inhibition on cellulose degradation as pointed out by Bezerra and Dias [9]. Hence, in order to make the SSCF model more realistic, this study introduces an inhibition effect of ethanol in the kinetics for the enzymatic hydrolysis pathway of cellulose to produce cellobiose. Philippidis et al. [10] showed that the value of the inhibition coefficient of ethanol on cellulose (conversion to cellobiose) is approximately 10 times higher than the inhibition coefficient of cellobiose on cellulose conversion. Therefore, the value of the inhibition constant of cellobiose on cellulose proposed by Kadam et al. [4] for the enzymatic hydrolysis of cellulose to cellobiose was multiplied by a factor 10 in order to obtain the inhibition constant for ethanol. With respect to ethanol inhibition on cellobiose hydrolysis, some authors [9,10] have concluded that inhibition by ethanol on cellobiose hydrolysis is insignificant in comparison with the inhibition effects of glucose on cellobiose depolymerization. Furthermore, for ethanol concentrations less than 4 M (equivalent to 18.42% wt/v ethanol) no significant inhibition of ethanol on the enzymatic activities in the saccharification was found [11]. The inhibition of ethanol on the cellobiose to glucose (and thus on the cellulose to glucose reaction pathway) was therefore neglected. Thus, only the mathematical expression for cellulose decomposition to cellobiose (eq. 1) is modified by adding an additional ethanol inhibition factor C_{Et}/K_{1Iet} as follows:

$$r_1 = \frac{k_{1r} C_{E_{1B}} R_S C_S}{1 + \frac{C_{G_2}}{K_{1IG2}} + \frac{C_G}{K_{1IG}} + \frac{C_{Xy}}{K_{1IXy}} + \frac{C_{Et}}{K_{1IEt}}} \tag{16}$$

As can be observed, the measurement units are different in the separate hydrolysis and co-fermentation models (see above). To resolve this issue, it is assumed in the mathematical model for the SSCF process that the density of the mixture is equal to 1 kg/L, such that both models can be integrated. The values and description of the parameters employed in the mathematical model can be found in the nomenclature section.

3 DYNAMIC SIMULATION OF THE SSCF MATHEMATICAL MODEL USING THE NREL PROCESS

3.1. NREL process

The process configuration of NREL (2002) presented in figure 1 is employed to test the proposed mathematical model for the SSCF unit operation in fed-batch mode. The SSCF unit is fed continuously with the slurry produced in the pretreatment section. The effluent from the SSCF reactor passes through a solid-liquid separator where the liquor is sent to further downstream processing (not shown).

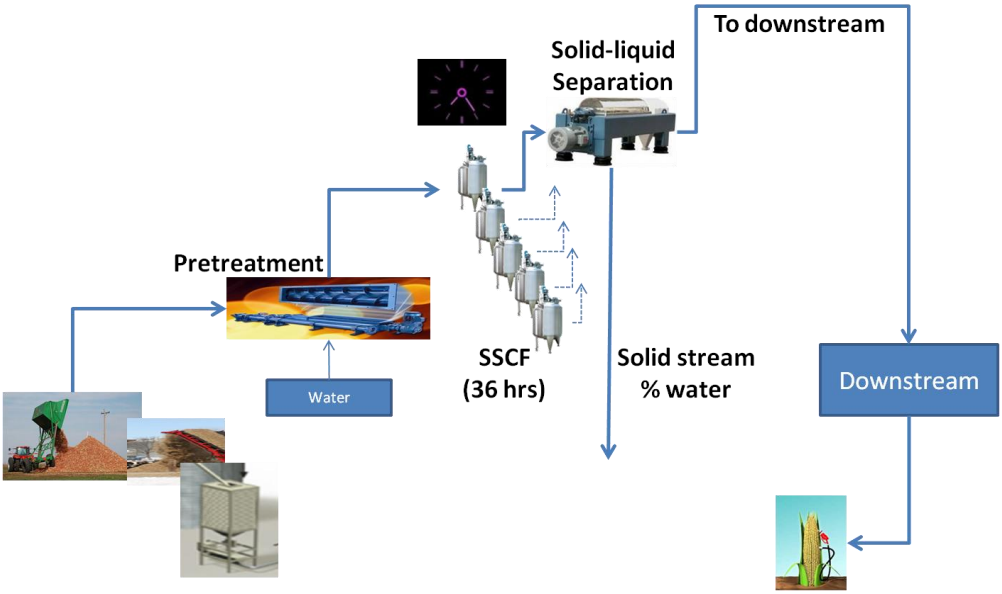

Figure 1. Process flowsheet for the dynamic simulation of a bioethanol production plant used in this work, involving dilute acid pretreatment and the SSCF unit.

This study uses a modified version of the NREL process which takes into account the pretreatment section and SSCF unit operation. The

mathematical model for pretreatment, which describes the breakdown of the structure of the lignocellulose matrix of the raw biomass in a continuous reactor, is taken from the work of Lavarack et al. [12]. This mathematical model predicts the decomposition of the most important cellulosic and hemicellulosic compounds such as glucan (cellulose), xylan, lignin and arabinan, by the action of diluted sulfuric acid. Consequently, the effluent from the pretreatment is fed continuously at the same flow rate to the SSCF as the effluent rate from the pretreatment reactor for 12 hrs followed by 36 hrs of reaction period.

The mass balance for the fed-batch operation of the SSCF unit can be represented in its generic form as follows:

$$V\frac{dC_i}{dt} = Q_{in}C_{in,i} + r_{i,j}V - C_i\frac{dV}{dt} \tag{17}$$

where, Q_{in} is the feed flow rate, $C_{in,i}$ is the concentration of compound i in the feed, $r_{i,j}$ is the rate of generation/degradation of compound i in the reaction j, V is the reactor volume, and C_i is the actual concentration of compound *i* in the reactor, which will be equal to the concentration in the outlet during the drawing period of the reactor.

As far as reaction volume is concerned, this is described as follows:

$$\frac{dV}{dt} = Q_{in} \tag{18}$$

3.2. Simulation platform

The simulation of the modified NREL process flowsheet for bioethanol production has been solved using the object-oriented MatLab/Simulink platform [13] as shown in figure 2. This type of implementation was chosen since it allows addressing several important issues during the simulation of the process flowsheet: (1) scheduling to realize the combination of unit operations in fed-batch and continuous in the simulation model; (2)

obtaining reliable results from the plant-wide operational point of view; (3) straightforward implementation of control strategies and introduction of process disturbances to analyze the responses in the whole process.

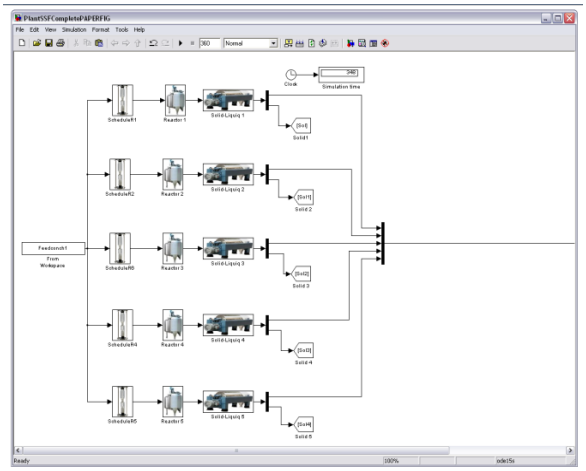

Figure 2. Simulation model for bioethanol production in Matlab Simulink.

3.3. Data

The input data employed to carry out the simulation were mostly taken from the NREL report. The main data related to feedstock composition employed for the simulation of the process flowsheet are shown in table 3. This simulation uses corn stover as a feedstock (using biomass composition for corn stover), but the mathematical model allows the simulation of different feedstocks by employing the corresponding values of biomass concentration of other cellulosic feedstocks.

Table 3. Main feedstock characteristics used in the simulation.

Feedstock*	Corn Stover
Dry feedstock capacity*	2352 MT/day
	% Dry biomass composition
Glucan (cellulose)*	37.4
Xylan*	21.1
Arabinan*	2.9
Lignin*	18
Ash*0	5.2
Other compounds	15.4

*NREL Report [3].

The information regarding the pretreatment and SSCF unit operation can be found in table 4 and table 5, respectively.

Table 4. Process conditions in the pretreatment.

Reactive compound *	Diluted sulfuric acid
Concentration % (wt/v)*	1.1
Residence time*	2 minutes
Temperature	170 °C
Solids in the reactor % (wt/wt)*	30
Feed flow rate	327696.66 kg/hr

*NREL Report [3].

Table 5. Process conditions in the SSCF unit.

Temperature	35°C
Inoculum level*	10%
Size of the vessels*	3596 m^3 (each)
Enzymes	Cellulases (EG, CBH and BDG)
Organism	*Saccharomyces cerevisiae* strain1400 (pLNH33)
Operating time	48 hr

*NREL Report [3].

3.4. Simulation results for SSCF unit

Following the simulation of a fed-batch SSCF unit, Figure 3 shows the simulated concentration profiles for: a) glucose, xylose, cellulose, ethanol and yeast, b) insoluble solids, c) cellobiose, and d) reactor volume of the SSCF unit.

It is considered that the initial concentrations for the inoculum correspond to the final concentrations of a previous fed-batch operation of the same reacting system. The plots clearly show the fed-batch operation in the reactor, especially in the reaction volume profile of the SSCF unit, where the feed flow to the reactor is applied during the first twelve hours of operation followed by an additional 36 hrs reaction period.

The concentration profiles inside the reactor can be divided in three main sections: before t = six hours, between six and twelve hours, and after the feed addition has finished after t = twelve hours.

During the first six hours of operation, corresponding to the first part of the substrate feeding period, it is observed that the cellulose concentration increases abruptly due to the feeding of fresh raw material, while the

glucose, xylose and cellobiose concentrations increase gradually as a consequence of the cellulose degradation taking place. Even though glucose and xylose are already present in the mixture, the drop in ethanol concentration is due to the feed rate being higher than the fermentation rate in this first period (t < six hours).

Between six and twelve hours, cellulose starts to be diluted despite of the fact that the loading period is not finished. The main reason is that significant ethanol production takes place in this period while glucose, xylose and cellobiose production due to cellulose hydrolysis is also ongoing.

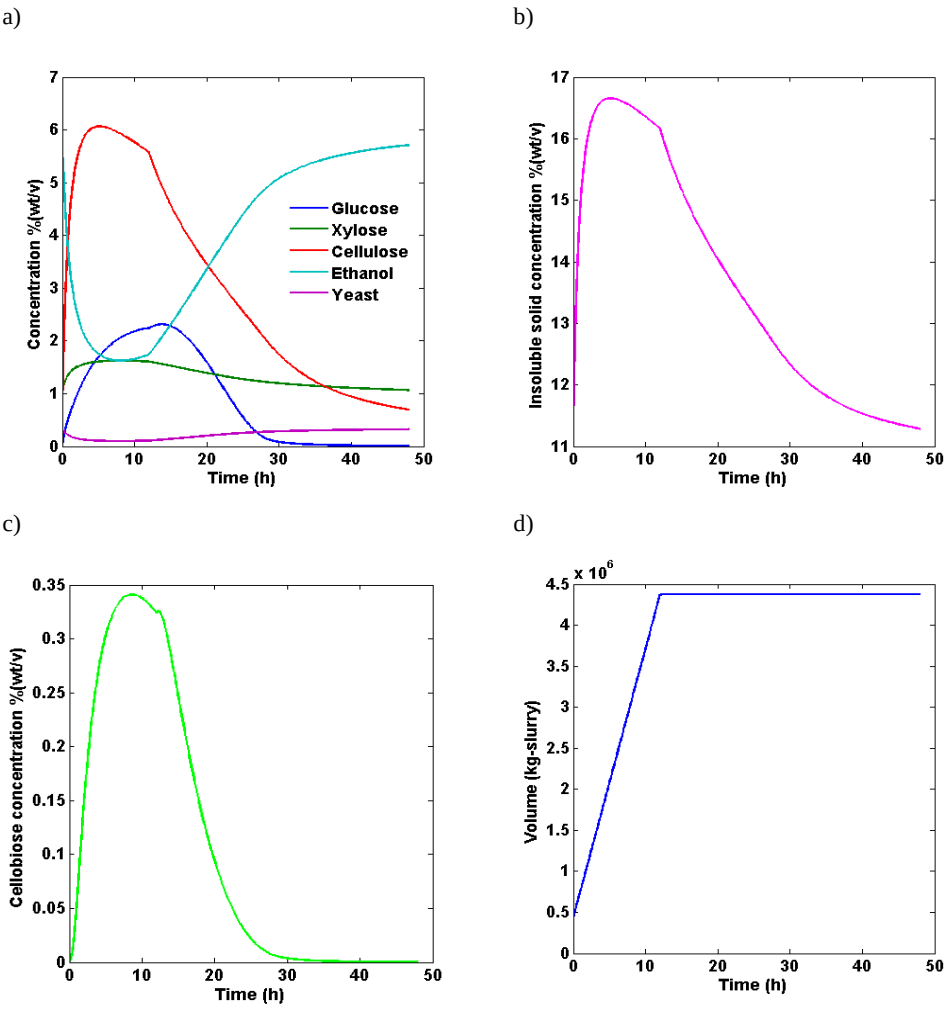

Figure 3. Concentration profiles in the SSCF unit for: a) Glucose, xylose, cellulose, ethanol and yeast, b) insoluble solids and c) cellobiose; d) volume profile for the SSCF unit.

Once the loading period has finished (after t = twelve hours), the cellulose concentration decreases faster, which is reflected slightly in the production

of glucose which also passes through a concentration maximum. Ethanol production is the most important result in this period: the ethanol production continues until the reaction time is finished. At the end of the reaction period, the figure shows that glucose and cellobiose have almost completely been converted, which is not the case for the cellulose and xylose. As far as cellulose is concerned, perhaps an inhibition effect owing to the presence of ethanol decreases the cellulose conversion. With respect to xylose, it is possible that the recombinant microorganisms cannot carry out a further conversion of this pentose to ethanol due to substrate inhibition is presented, being this higher compared with glucose inhibition on ethanol production. The insoluble solids profile can be explained similarly to the cellulose profile, because the cellulose is the only compound being degraded among the compounds in the solid phase.

Finally, table 6 shows the results for the concentration of the main components of the SSCF unit outflow after completion of a fed-batch operation. The results show that obtained ethanol concentration (5.71 % wt/v) is found in the normal range when not high concentration of insoluble solids is in the reactor.

Table 6. Concentrations for the SSCF output.

Component	% (wt/v)
Glucose	0.01
Xylose	1.06
Cellulose	0.69
Ethanol	5.71
Yeast	0.32
Insoluble solids	11.28

5 CONCLUSIONS

A mathematical model for simultaneous saccharification and co-fermentation (SSCF) has been developed in this study. Model construction has been carried out by combining two existing and already validated mathematical models for enzymatic hydrolysis and co-fermentation respectively. An inhibition of ethanol on cellulose conversion was introduced coupling the two models in order to increase the

degree of reliability of the resulting SSCF model.

The SSCF mathematical model has been tested using the NREL process configuration and data. The test was carried out via dynamic simulation of the pretreatment and SSCF units working in continuous and fed-batch operation, respectively.

Even though the mathematical model for the SSCF unit is not completely verified by experimental results, the basis for the construction of the model is theoretically sustained in previous research. Of course, the model is still open for further verification by experimental results and statistical analysis.

ACKNOWLEDGEMENTS

The authors of this paper acknowledge the Mexican National Council for Science and Technology (CONACyT) and the Danish Research Council for Technology and Production Sciences (FTP # 274-07-0339) for the financial support of this project.

NOMENCLATURE

E_a	Activation energy = -5540 cal/mol
C_{E_T}	Total enzyme concentration, g/kg
$C_{E_{1B}}$	Bound concentration of CHB and EG, g/kg
$C_{E_{2B}}$	Bound concentration of β-glucosidase, g/kg
C_{E_F}	Free enzyme concentration, g/kg
$C_{E_{2F}}$	Concentration of β-glucosidase in solution, g/kg
$E_{1\max}$	maximum Maximum mass of enzyme 1 that can be adsorb onto a unit mass of substrate, 0.06 $g\ protein/g\ substrate$.
$E_{2\max}$	Maximum mass of enzyme 2 that can be adsorb onto a unit mass of substrate, 0.01 $g\ protein/g\ substrate$.
C_{Et_G}	Ethanol concentration from glucose fermentation
$C_{Et_{Xy}}$	Ethanol concentration from xylose fermentation
$Et_{\max,G}$	Ethanol concentration above which cells do not grow in glucose fermentation, $95.40\ for\ \mathrm{Et} \le 95.4\ g/L$, $129.90\ for\ 95.4 < Et \le 129.9\ g/L$
$Et_{\max,Xy}$	Ethanol concentration above which cells do not grow in xylose fermentation = 59.040 g/L
$Et'_{\max,G}$	Ethanol concentration above which cells do not produce ethanol in glucose fermentation $103\ for\ \mathrm{Et} \le 103\ g/L$, $136.40\ for\ 103 < Et \le 136.4\ g/L$
$Et'_{\max,Xy}$	Ethanol concentration above which cells do not produce ethanol in xylose fermentation = 60.20 g/L
C_G	Glucose concentration, g/kg
C_{G_2}	Cellobiose concentration, g/kg
$K_{1\mathrm{ad}}$	Dissociation constant for enzyme 1 = 0.4 $g\ protein/g\ substrate$
$K_{2\mathrm{ad}}$	Dissociation constant for enzyme 2 = 0.1 $g\ protein/g\ substrate$
k_{1r}	Reaction rate constant 1 = 22.3 $g/mg \cdot h$
k_{2r}	Reaction rate constant 2 = 7.18 $g/mg \cdot h$
k_{3r}	Reaction rate constant 3 = 285.5 h^{-1}
K_{1IG}	Inhibition constant for glucose 1 = 0.1 g/kg
K_{2IG}	Inhibition constant for glucose 2 = 0.04 g/kg
K_{3IG}	Inhibition constant for glucose 3 = 3.9 g/kg
K_{1IG2}	Inhibition constant for cellobiose 1 = 0.015 g/kg
K_{2IG2}	Inhibition constant for cellobiose 2 = 132.0 g/kg
K_{1IEt}	Inhibition constant for ethanol 1 = 0.15 g/kg
K_{1IXy}	Inhibition constant for xylose 1 = 0.1 g/kg
K_{2IXy}	Inhibition constant for xylose 2 = 0.2 g/kg
K_{3IXy}	Inhibition constant for xylose 3 = 201.0 g/kg
K_{3M}	Substrate (cellobiose) saturation contant = 24.3 g/kg
K_{4G}	Monod constant, for growth on glucose = 0.565 g/L
K_{5Xy}	Monod constant, for growth on xylose =3.4 g/L
K'_{8G}	Monod constant, for product formation from glucose = 1.342 g/L
K'_{9Xy}	Monod constant, for product formation from xylose = 3.4 g/L
K_{4IG}	Inhibition constant, for growth on glucose = 283.7 g/L

K_{5IXy}	Inhibition constant, for growth on xylose = 18.1 g/L
$K_{8IG}^{'}$	Inhibition constant, for product formation from glucose = 4890.0 g/L
$K_{9IXy}^{'}$	Inhibition constant, for product formation from xylose = 81.30 g/L
m_G	Maintenance coefficient in glucose fermentation = 0.097 h^{-1}
m_{Xy}	Maintenance coefficient in xylose fermentation =0.067 h^{-1}
r_i	Reaction rate, $g/kg \cdot h$ = $g/L \cdot h$, $\rho_{mixture} = 1\ kg/L$
$r_{X,TOT}$	Total reaction rate for the biomass, $g/L \cdot h$
$r_{Et,TOT}$	Total reaction rate for ethanol, $g/L \cdot h$
R	Universal gas constant, 1.9872 $cal/mol \cdot K$
R_S	Substrate reactivity
C_S	Substrate concentration, g/kg
T	Temperature, K
C_{Xy}	Xylose concentration, g/kg
X_G	Cell dry weight in glucose fermentation, g/L
X_{Xy}	Cell dry weight in xylose fermentation,
x_i	Mass fraction of glucose or xylose in the glucose and xylose mixture = $x_G / (x_G + x_{Xy})$ and $x_{Xy} / (x_G + x_{Xy})$.
$Y_{Et_G/G}$	Product yield constant (g-ethanol/g-glucose) = 0.470 g/g
$Y_{Et_{Xy}/Xy}$	Product yield constant (g-ethanol/g-xylose) = 0.400 g/g
$Y_{X_G/G}$	Cell yield constant from glucose (g-cells/g-substrate) =0.115 g/g
$Y_{X_{Xy}/Xy}$	Cell yield constant from xylose (g-cells/g-substrate) =0.162 g/g
α	Constant relating substrate reactivity with degree of hydrolysis, 1.
β_G	constants in product inhibition model in glucose fermentation 1.29 *for* $Et \le 95.4\, g/L$, 0.25 *for* $95.4 < Et \le 129.9\, g/L$
β_{Xy}	Constant in the product inhibition model in xylose fermentation = 1.036 g/L
γ^G	Maximum specific rate of glucose formation 1.42 *for* $Et \le 95.4$ g/L,
γ^{Xy}	Maximum specific rate of xylose formation = 0.608 g/L
$\mu_{max,G}$	Maximum specific growth rate in glucose fermentation = 0.662 h^{-1}
$\mu_{max,Xy}$	Maximum specific growth rate in xylose fermentation = 0.190 h^{-1}
$\nu_{max,G}$	Maximum specific rate of glucose formation = 2.005 h^{-1}
$\nu_{max,Xy}$	Maximum specific rate of xylose formation = 0.250 h^{-1}

REFERENCES

1 Liquid Transportation Fuels from Coal and Biomass: Technological Status, Costs, and Environmental Impacts. 2009, The National Academy press. Washington, DC. USA.

2 Hayes, D.J., "An examination of biorefining processes, catalyst and challenges". *Catalysis Today*,**145**, 138-151 (2009).

3 Aden, A., Ruth, M., Ibsen, K., Jechura, J., Neeves, K., Sheehan, J., Wallace, B., Montague, L., Slayton, A., Lukas, J., "Lignocellulosic Biomass to Ethanol Process Design and Economics Utilizing Co-Current Dilute Acid Prehydrolysis and Enzymatic Hydrolysis for Corn Stover". *National Renewable Energy Laboratory Technical Report*. NREL/TP-510-32438 (2002).

4 Kadam, K.L. Rydholm, E.C. McMillan, J.D., "Development and Validation of a Kinetic Model for Enzymatic Saccharification of Lignocellulosic Biomass". *Biotechnology Progress*, **20**, 698-705 (2004).

5 Sin, G., Meyer, A.S., Gernaey, K.V., "Assessing reliability of cellulose hydrolysis models to support bioefuel process design-identifiability and uncertainty analysis". *Computers and Chemical Engineering.* **doi:**10.1016/j.compchemeng.2010.02.012 (2010).

6 Hodge, D.B., Karim, M.N., Schell, D.J., McMillan, J.D., "Model-Based Fed-Batch for High-Solids Enzymatic Cellulose Hydrolysis". *Applied biochemistry and biotechnology*. **152**, 88-107 (2009).

7 Morales-Rodriguez, R., Capron, M., Huusom, J.K., Sin, G., "Controlled fed-batch operation for improving cellulose hydrolysis in 2G bioethanol production". Accepted manuscript for ESCAPE 20 (20th *European Symposium on Computer Aided Process Engineering*). 6-9 of July (2010). Naples, Italy.

8 Krishnan, M.S., Ho, N.W.Y., Tsao, G.T., "Fermentation Kinetics of Ethanol production from Glucose and Xylose by recombinant Saccharomyces 1400(pLNH33)". *Applied biochemistry and biotechnology*, **77-79**, 373-388 (1999).

9 Bezerra, R.M.F., Dias, A.A., "Enzymatic Kinetic of Cellulose Hydrolysis". *Applied biochemistry and biotechnology*. **126**, 49-59 (2005).

10 Philippidis, G.P., Smith, T.K., Wyman, C.E., "Study of the Enzymatic Hydrolysis of Cellulose for Production of Fuel Ethanol by the Simultaneous Saccharification and Fermentation Process". *Biotechnology and Bioengineering*. **41**, 846-853 (1993).

11 Ooshirna, H., Ishitani., Y., Har, Y., "Simultaneous Saccharification and Fermentation of Cellulose: Effect of Ethanol on Enzymatic Saccharification of Cellulose". *Biotechnology and Bioengineering*. **27**, 389-397 (1985).

12 Lavarack, B.P., Griffin, G.J., Rodman, D., "The acid hydrolysis of sugarcane bagasse hemicelluloses to produce xylose, arabinose, glucose and other products". *Biomass and bioenergy*, **23**, 367-380 (2002).

13 MatLab/Simulink. The MathWorks, Inc. 2008. Version 7.7.0.471 (R2008b)